Electronic Absorption Spectra of HXeCl, HXeBr, HXeI, and HXeCN in Xe Matrix

Jussi Ahokas, Kari Vaskonen, Jussi Eloranta, and Henrik Kunttu*

Department of Chemistry, University of Jyväskylä, P.O. Box 35, Fin-40351 Jyväskylä, Finland

Received: June 13, 2000; In Final Form: August 10, 2000

The electronic UV absorption spectra of thermal reaction products H−Xe−Y (Y= Cl, Br, I, or CN) have been measured in solid Xe at 12 K. The spectra are obtained after the annealing of an extensively irradiated matrix doped with an HCl, HBr, HI, or HCN precursor. The spectral assignment is based on the correlation between the UV spectra and the known infrared absorptions of these compounds. An analysis of the annealing behavior of the UV absorptions due to H−Xe−Y, Y/Xe and H/Xe yields a quantitative estimate that 20−30% of the photogenerated Y is converted to H−Xe−Y. Present multireference configuration interaction (MRCI) calculations provide strong support that the spectral observations are due to the $A\ ^1\Sigma \leftarrow X\ ^1\Sigma$ transitions of H−Xe−Y. The spectral width of the absorptions indicate that the transitions are from a bound ground state to a repulsive excited state.

Introduction

Group VIII, the noble gases (Ng), forms the end of the periodic table of the elements. Their electronic structures suggest chemical inertness and, indeed, until the 1960s, no noble gas compounds were known.[1] Quite impressively, the existence of covalent fluorides of both xenon and krypton were predicted as early as 1933 by Pauling.[2] At present, some tens of stable neutral Xe and Kr compounds have been synthesized. Extending the view to cover ionic species increases the number of known noble gas containing compounds significantly. Moreover, the lighter noble gases, Ar, Ne, and He, also possess a chemical role in the charged species. Well-known examples of such strong binding are the protonated noble gases NgH^+ [3] and their solvated forms, the proton bound noble gas dimers Ng_2H^+.[4,5]

It has been known for quite some time that solid noble gas matrices, besides providing an inert environment for isolating chemical species of interest, can be utilized as ideal media for studies of chemical reactivity.[6,7] A fascinating outcome of such studies is that in favorable circumstances the isolating "inert" noble gas atoms show enhanced reactivity. An extensive series of investigations by Räsänen et al. starting from the mid 90's has shown that the chemistry of noble gases is, in fact, much richer and diverse than originally expected.[8,9] An entire family of new noble gas containing molecules of a common form H−Ng−Y has been characterized in straightforward experiments based on UV photolysis of a HY precursors and subsequent thermal activation of the hydrogen atoms produced in the photolysis. Y is typically an atom or a molecular group of relatively high electron affinity and Ng is Kr or Xe. A rather peculiar exception of this rule is the xenon dihydride molecule, H−Xe−H, which is formed in xenon matrices doped with atomic hydrogen. Very recently, formation of the first neutral argon compound H−Ar−F was verified in a VUV photolyzed HF/Ar matrix.[10]

The novel H−Ng−Y molecules possess significant charge transfer character on their ground electronic surface, and thus, strong vibrational transitions are expected. Indeed, the existence of these molecules relies entirely on the infrared (IR) observations. Although the electronic states of H−Ng-Y have received some recent theoretical interest,[11] the electronic absorption spectra have not been reported. However, indirect evidence of exceptionally strong electronic transitions can be extracted from their efficient photodissociation.[8] In this study, we present spectral data on the UV absorptions observed in HCl, HBr, HI, and HCN doped xenon matrices. The experiment relies on 193 nm photolysis of the precursors and absorption measurement with a deuterium lamp imaged on a charge-coupled device (CCD) detector. Annealing of the photolyzed samples near 45 K causes rather dramatic changes in the spectra, simultaneously with the decrease of the H/Xe absorption near 200 nm,[12] a very strong broad absorption feature appears in the 250 nm − 320 nm range. On the basis of comparison with the IR measurements and the predictions of multireference configuration interaction (MRCI) calculations, we suggest that these absorptions belong to the H−Xe−Y molecules.

Experimental Section

The gas samples were prepared in a 1 dm^3 Pyrex sample bulb connected to an all glass vacuum manifold evacuated to 3×10^{-7} mbar with a diffusion pump. Two capacitance manometers (MKS Instruments) were used to obtain accurate guest-to-host ratios. For all samples, this ratio was 1:1000 with an exception of HI/Xe, where the ratio was approximately 1:300. In the latter case, it was difficult to obtain an accurate matrix ratio because HI is effectively adsorbed to the walls of the vacuum manifold. The xenon solids doped with HCl, HBr, HI, and HCN were grown in a closed cycle cryostat (APD Cryogenics, Inc., DE−202) with the lowest accessible temperature near 12 K. The temperature at the cryotip was measured with a silicon diode and controlled with a Lake Shore 330 controller unit. The cryostat was connected to a stainless steel vacuum system pumped with a turbomolecular pump near 3×10^{-7} mbar. The premixed gas mixture was admitted to the cryostat via a 1/16 in. stainless steel capillary.The deposition rate was controlled with a needle valve and a capacitance manometer. Typically,

* To whom correspondence should be addressed. E-mail: Henrik.Kunttu@jyu.fi

10.1021/jp002141t CCC: $19.00
Published on Web 10/04/2000

10−20 mbar was deposited from 1 dm^3 volume and 350 mbar backing pressure in 10 min. To produce monomeric trapping of the precursor molecules, the MgF_2 substrate was held at 20 K during deposition. After deposition, the sample was briefly annealed at 45 K. Solid films grown under these conditions showed some cracks and slight haziness after heating, which affected their optical quality.

IR spectra of the matrix samples were recorded with a Nicolet Magna IR 760 FTIR spectrometer equipped with a HgCdTe detector and a KBr beam splitter. The MgF_2 substrate limited the transparent spectral range to >850 cm^{-1}. The outer cryostat windows in the IR measurements were CsI. The UV absorption spectra were obtained with a spectrometer composed of a 30 W deuterium source, a 15 cm spectrograph (Acton SP 150), and a CCD camera (Princeton Instruments). The exposure time of the detector was controlled with an electrical shutter. The cutoff of the quartz window of the CCD put a lower limit of detection near 190 nm. Atomic lines of mercury were used for wavelength calibration. Background spectra were recorded through the unphotolyzed samples. To keep the background stable in the subsequent irradiation-annealing cycles, it was essential to carefully anneal the sample near 45 K prior to starting the photolysis. A 193 nm (ArF) excimer laser (Lambda Physik Optex) with a pulse energy of 5−12 mJ was used to photolyze the samples.

HCl and HBr of 99.8% purity were obtained from Messer Griesheim and Cambridge Isotope Laboratories, respectively. HCN was synthesized in a vacuum line from KCN and sulfuric acid, dried with P_2O_5, and trapped at liquid nitrogen temperature. HI was synthesized from water, iodine, and red phosphorus.[13] Xenon (99.997%) was obtained from AGA.

Computational Methods

The geometries of the H−Xe−Y ground-state molecules were optimized by using the RCISD method with linear geometry restriction. The RCISD method consists of spin restricted Hartree−Fock (RHF) method with a subsequent configuration interaction treatment involving single and double substitutions (CISD).[14] Further calculations were performed at the optimized ground-state geometry for the ground state and the first excited state of A_1 symmetry within the C_{2v} point group. In this treatment, the initial orbitals were first obtained with RHF and refined in a multi-configuration self-consistent field (MCSCF) calculation employing the complete active space (CAS) orbitals.[15] The active space included 8 electrons and 6 orbitals in A_1 symmetry of C_{2v}. No orbitals were frozen in the A_1 symmetry, whereas all B_1 and B_2 orbitals were frozen. Both states were calculated simultaneously by using the state averaging method. Finally, an internally contracted configuration interaction calculation (ICMRCI) with single and double excitations was carried out based on the MCSCF orbitals.[16] The obtained energies were all subject to the multireference analogue of the Davidson's size-consistency correction.[17] The ground and excited dipole moments and Mulliken partial charges as well as transition dipole moments were obtained by standard methods.[18]

The basis set used for hydrogen was Dunning's cc-pVDZ,[19] whereas for Xe and the halogens (Cl, Br, and I), we rely on the effective core potential (ECP) basis sets developed by the Stuttgart group.[20] This combination was chosen to obtain good balance between the hydrogen and halogen basis sets. The geometry optimizations were performed with GAUSSIAN 98 program[21] and the ICMRCI calculations with the MOLPRO 2000 package[22] on GNU/LINUX systems.

Results

IR Observations. The relatively thin matrices grown for measurements in the UV do not provide high signal-to-noise (S/N) ratios in the less sensitive mid-IR. However, for all of the samples, monomeric trapping of the precursor and, most importantly, formation of the previously characterized strong H−Xe−Y absorptions was verified upon annealing the samples near 45 K. The HCl monomer absorption is centered at 2858 cm^{-1} with a shoulder at 2856 cm^{-1}. A very weak dimer absorption was observed near 2818 cm^{-1}. All absorptions due to HCl were efficiently photobleached at 193 nm, and within ∼ 1000 laser pulses (12 mJ cm^{-2}), the photolysis was nearly complete. In accordance with the observations by Pettersson and co-workers,[23] new absorptions at 1648 and 1166 cm^{-1} due to H−Xe−Cl and H−Xe−H appeared upon annealing. These absorption features disappeared completely in 10 min photolysis with an unfiltered D_2 lamp or, alternatively, by few laser pulses at 193 nm. Subsequent annealing of the sample regenerated the absorptions nearly with their original intensities.

After preparation of a HBr/Xe matrix, characteristic IR absorptions were observed at 2567 , 2532 , and 2509 cm^{-1}. Although practically no absorptions due to dimers or trimers were present immediately after deposition, annealing of the matrix at 45 K caused weak dimer and trimer peaks to appear. After few hundred pulses at 193 nm, 100% of the precursor was dissociated. Upon annealing the sample at 45 K, new absorptions appeared at 1504, 1500, and 1487 cm^{-1}. These absorptions have been previously ascribed to the H−Xe−Br molecule.[23] In a subsequent photolysis with an unfiltered D_2 lamp these signals were photobleached in ca. 10 min and recovered nearly with their original intensities upon a second annealing cycle.

The IR measurement of a 1:300 HI/Xe matrix showed a monomer absorption at 2215 cm^{-1} and a broad structureless feature at 2208−2202 cm^{-1}. Additional absorptions at 2166, 2161, and 2146 cm^{-1} belong to dimer and trimers. Due to the low deposition temperature, HI was well isolated in the solid Xe samples, and the contribution of dimers and trimers was relatively small. However, the amount of dimers and trimers increased considerably when the sample was heated to 45 K. At 193 nm photolysis, the IR absorptions of HI disappeared within some hundreds of laser pulses. Upon thermal cycling, 12−45−12 K, new thermally induced absorptions due to H−Xe−I appeared at 1213, 1193, and 1187 cm^{-1}.[23] These absorptions can be bleached by few hundred 193 nm laser pulses or 10 min. irradiation with unfiltered D_2 lamp, and partially regenerated after a new annealing cycle.

Under the present experimental conditions nearly perfect isolation of HCN was achieved. The only absorptions observed in the CH stretching region, 3276 and 3279 cm^{-1}, are due to the monomer.[24] By annealing the sample to 45 K, weak dimer bands appeared at 3268 and 3191 cm^{-1}. In the UV photolysis, the dimer bands disappeared completely and only ∼ 30% of the monomer was left after 1500 pulses. The higher dissociation efficiency of matrix isolated dimers and oligomers was recently discussed by Bondybey et al.[25] Simultaneously, with the decrease of the precursor absorptions, a very weak 2049 cm^{-1} band of CN radical[26] appeared. The S/N ratio was not sufficient for observation of HCN to HNC photoisomerization in the present thin matrices. Again, annealing of the photolyzed sample reproduced the previously reported spectral changes, i.e., the appearance of new bands due to H−Xe−CN, H−XeNC, and H−Xe−H at 1624, 1851, and 1166 cm^{-1}, respectively.[26] All

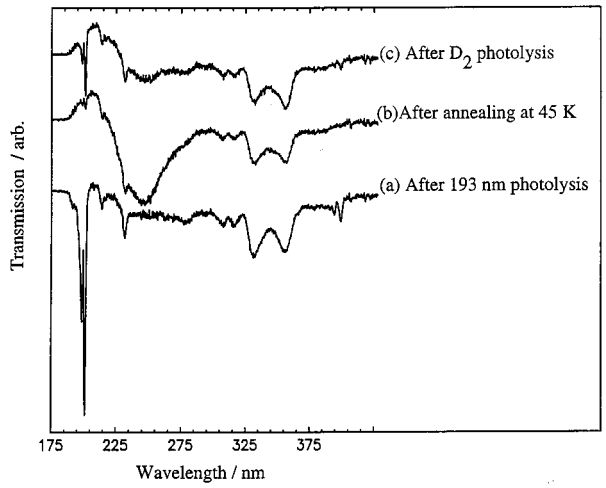

Figure 1. UV absorption spectrum of a HCl/Xe 1:1000 matrix. The absorptions observed after 193 nm photolysis are due to H/Xe (200 nm) and Cl/Xe (335 nm). The broad feature in the middle spectrum is assigned to H−Xe−Cl molecule.

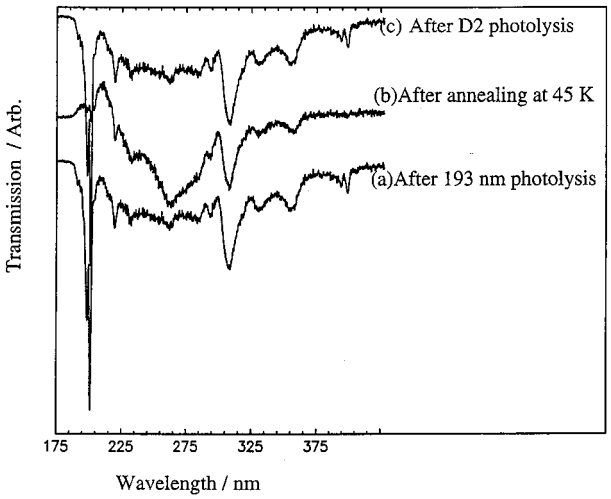

Figure 2. UV absorption spectrum of a HBr/Xe 1:1000 matrix. The absorptions observed after 193 nm photolysis are due to H/Xe (200 nm) and Br/Xe (300 nm). The broad feature in the middle spectrum is assigned to H−Xe−Br molecule.

these absorptions could be photobleached and partially regenerated in subsequent irradiation-annealing cycles.

UV Observations. Figure 1 shows UV absorption spectra of an extensively photolyzed HCl/Xe matrix. The most prominent absorptions are the sharp bands at 198 and 201 nm, which can be assigned to the two lowest energy components of the absorption progression of the caged H atom.[12] The broad 356 and 331 nm bands and the weaker features near 307 and 316 nm are identical to what is seen in the excitation spectra of the triatomic $Xe_2^+Cl^-$ exciplex emission in extensively irradiated Cl_2 or HCl doped Xe solids.[27] For comparison, the $B \leftarrow X$ and $D \leftarrow X$ absorptions of XeCl in argon matrix are at 338 and 253 nm, respectively.[28] With these numbers in mind the observed 231 nm absorption seems too much blue shifted to belong to XeCl, and we leave this peak, and the one at 214 nm unassigned. The most striking change in the spectrum upon annealing the sample at 45 K is the nearly complete disappearance of the H/Xe absorption and a simultaneous growth of a very strong, structureless absorption centered at ca. 246 nm. The full width at half the maximum (fwhm) of this band is 65 nm, which corresponds to 0.7 eV. Other changes in the spectrum are related to the XeCl absorptions, which decrease by ca. 28%. Irradiation of the annealed sample with the full spectrum of a D_2 lamp or with a 193 nm laser caused complete disappearance of the 246 nm band, full recovery of the XeCl $B \leftarrow X$ absorption and ca. 20% recovery of the H/Xe absorptions (Figure 1).

As seen in Figure 2, the spectral observations in the photolyzed HBr doped Xe matrix are quite similar to the HCl/Xe case. The photolysis produced strong H/Xe absorptions and a broad band centered at 308 nm. Comparison with the excitation spectra of $Xe_2^+Br^-$ emission in Br doped Xe[27] and the absorption spectrum of XeBr in Ar[28] yields a straightforward assignment that this absorption, and its weaker blue shifted satellites are due to the $B \leftarrow X$ system of XeBr. Again, we observe two unassigned absorptions near 220 and 230 nm. By annealing the sample at 45 K, the H/Xe absorptions disappeared and a broad structureless band was formed at 262 nm. Once formed in annealing, this absorber is efficiently photolyzed with a D_2 lamp or 193 nm laser. Simultaneously, partial recovery of the H/Xe absorptions is observed.

A photolyzed HI/Xe sample showed a prominent progression of UV absorptions near 280 nm and very weak atomic hydrogen absorptions at ca. 200 nm. The structure of the absorption system

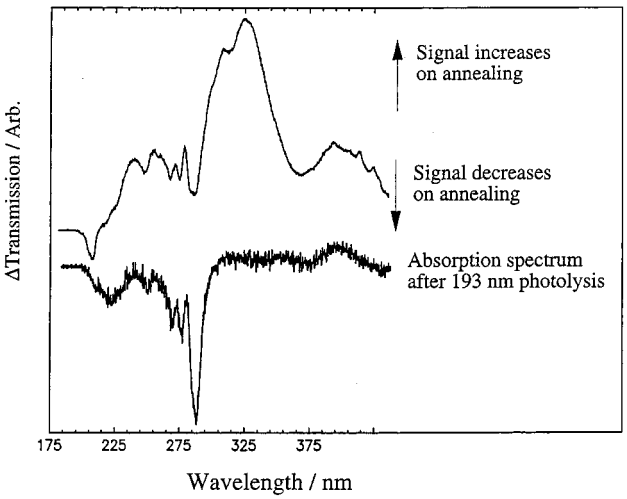

Figure 3. UV absorption spectrum of a HI/Xe 1:300 matrix. The lower spectrum shows the I/Xe absorption after 193 nm photolysis. The difference spectrum shows the growth of a broad absorption feature (300 nm) assigned to H−Xe−I.

at 280 nm corresponds very closely to the excitation spectrum of $Xe_2^+I^-$ emission in solid Xe.[27] Thus, we assign the 280 nm absorption system to charge transfer between Xe and atomic iodine. Because the charge transfer absorptions overlap strongly with the spectral region where the absorption due to H−Xe−I is expected, a difference between UV spectra recorded after photolysis and after subsequent annealing is presented in Figure 3. The main observations upon annealing at 45 K are the decrease of absorptions due to I/Xe and H/Xe, and appearance of a new broad feature centered at 315 nm. This absorption can be efficiently bleached with a D_2 lamp and partially regenerated by annealing at 45 K. Before proceeding, it is important to note that the intensity of the H/Xe absorption in a photolyzed HI/Xe matrix was significantly weaker than in other samples involving different precursor molecules and, apparently, only a very small amount of atomic hydrogen was available for formation H−Xe−I upon annealing. Consequently, the broad I/Xe and H−Xe−I absorptions possess comparable intensities and cannot be clearly separated from each other.

Figure 4 displays the UV absorption spectra of a 1:1000 HCN/Xe matrix after 30% photolysis of the precursor. In accordance with the hydrogen halide samples, photolysis yields very strong

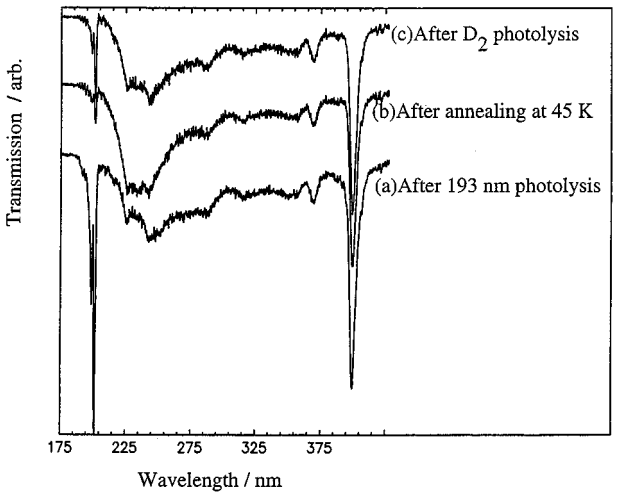

Figure 4. UV absorption spectrum of a HCN/Xe 1:1000 matrix. The absorptions observed after 193 nm photolysis are due to H/Xe (200 nm) and CN radical (400 nm). The broad feature in the middle spectrum is assigned to H−Xe−CN molecule.

H/Xe absorptions at 201 and 198 nm. In addition, strong bands at 400 and 369 nm appear. On the basis of previous absorption measurements by Bondybey et al.,[29] these bands can be assigned to the $B \leftarrow X$ transition of CN radical. In addition to these well-defined bands, a diffusive absorption with maxima at 226 and 242 nm develops in the photolysis. Again, annealing the sample at 45 K caused a nearly complete destruction of the H/Xe absorptions and growth of a broad band centered at 234 nm. Simultaneously, the CN radical absorption is diminished by ∼ 20%. Subsequent irradiation at 193 nm reduces the 234 nm band to its original intensity and recovers partially the H/Xe and CN absorptions.

Computational Results. All ground-state molecules H−Xe−Y, where Y = Cl, Br, or I, were first optimized on their singlet ground state. The considered compounds are linear with H−Xe and Xe−Y bond lengths varying as (1.68 Å, 2.70 Å), (1.70 Å, 2.84 Å), and (1.74 Å, 3.05 Å) for H−Xe−Cl, H−Xe−Br, and H−Xe−I, respectively. A vibrational analysis at the CISD level was performed to verify that these configurations represent minima on the ground-state potential energy surfaces. For HXeI and HXeBr, the obtained Xe−H stretching frequencies were 1637 and 1818 cm^{-1}, respectively. For a reason that is unclear, the two programs yielded different frequencies for HXeCl: 1907 cm^{-1} (GAUSSIAN), 1953 cm^{-1} (MOLPRO). The great sensitivity of the computed frequencies to basis set has previously been demonstrated for HXeY.[23] As the electron affinity of the halogen decreases from Cl to I, the H−Xe bond length increases and the positive partial charge on Xe decreases from 0.61 to 0.42. The hydrogen atom has a small positive partial charge in all compounds. Vertical excitation from the ground state to the first excited state of A_1 symmetry ($^1\Sigma$) yields a significant redistribution of charge density as shown in Table 1. This effect is most pronouncing in H−Xe−Cl, in which the direction of the dipole moment is reversed upon electronic excitation. The ground-state molecules all exhibit large dipole moments, which are then somewhat reduced in the first excited state. The transition dipole moments between the ground and the excited state are very large in all molecules as shown in the last column of Table 1. The overall trend is that the excitation energy decreases as the electron affinity of the halogen decreases. For a description of the multidimensional surfaces for the ground and excited states of H−Xe−Cl, we refer to the single reference computational study of ref 11.

TABLE 1: Summary of the MRCI Results for the Ground and First A_1 Excited State of H−Xe−Y Molecules[a]

compound	Δq(H)	Δq(Xe)	Δq(Y)	D_{gnd}	D_{exc}	E	Trm
HXeCl	−0.16	−0.05	+0.21	6.8	2.4	241(250)[b]	7.0
HXeBr	−0.08	−0.01	+0.09	6.2	3.9	262	7.5
HXeI	−0.01	+0.04	−0.03	5.6	5.2	288	8.1

[a] The Δq's are the Mulliken partial charge diferences between the ground and excited state, D_{gnd} is the ground-state dipole moment in Debye, D_{exc} is the excited-state dipole moment, E is the excitation energy of the first excited state in nm, and Trm is the electric transition dipole moment (Debye). [b] Single reference CISD calculation of ref 11.

Discussion

Because the thermally induced UV absorptions do not show any vibrational structure, their assignment relies entirely on comparison with the well-characterized IR absorptions of H−Xe−Y,[23,26] and the theoretical predictions of their electronic absorption spectra. It has, indeed, been shown in the present series of experiments that upon annealing a photolyzed Xe matrix doped with HY (Y═Cl, Br, I, or CN), besides a very intense ν(Xe−H) absorption in the 1400 cm^{-1} region, strong structureless UV absorptions in the 250−320 nm region are observed. The perfect correlation between the IR and UV absorptions in subsequent photolysis and annealing cycles would indicate that both absorptions are due to the same chemical species. The spectral width of the features in the UV suggest that these transitions are from a bound ground state to a repulsive excited state. Thus, the same transitions are most likely responsible for the rapid photodissociation observed in the previous experiments.[23,26] As seen in Figures 1−3, the intensities of the thermally induced absorptions clearly exceed those of the Cl/Xe, Br/Xe, and I/Xe exciplexes. This is consistent with our theoretical prediction of 7−8 D for the transition moments. These numbers should be compared with the ca. 2 D obtained for the halogen/Xe exciplexes by Dunning and Hay.[30]

Considering the spectral width of the UV absorptions, it may be estimated that the transition moment should be even higher than that of the H /Xe exciplex near 200 nm. We have recently estimated that a hydrogen atom trapped as an octahedral impurity in Xe would have a transition moment of 4 D.[31] On the basis of these arguments, and the fact that not all hydrogen and Y atoms react upon annealing to form the absorbing H−Xe−Y species, it is clear that the H−Xe−Y molecules do, indeed, possess UV absorptions of exceptional strength. Because the contribution of H−Xe−H on these spectra is not resolved, and may be dependent on the initial precursor, it is not possible to quantitatively compare the absorption strengths of various H−Xe−Y compounds with each other. However, a clear trend is that the absorption center shifts from 250 to 320 nm as the electron affinity of Y decreases. This observation suggests that the strong UV absorption may involve a charge transfer process, where the halogen atom acts as a charge donor. The electron affinities of Cl and CN are almost identical and, in accordance with this simple model, the absorptions are located approximately at the same wavelength.

The relative number of H−Xe−Y molecules responsible for the absorptions can be estimated from the reduction of Y upon annealing. When Y is a halogen atom, the Y/Xe exciplex absorption can be used as a probe. The amount of CN radicals can be monitored from the B ← X absorption of CN at 400 nm. Annealing a Xe matrix doped with H and Cl caused, in addition to appearance of the H−Xe−Cl absorption, 28% reduction of the Cl/Xe exciplex absorption and a complete disappearance of the absorption due to octahedrally trapped hydrogen atoms. If we assume that the initial photolysis produces H and Cl in

equal amounts, this means that 28% of atomic hydrogen present reacts with Cl to produce H−Xe−Cl or HCl, whereas the remaining 72% disappear via some other route. Possible channels responsible for the disappearance would involve trapping in substitutional lattice sites, formation of H−Xe−H, or formation of molecular hydrogen. It is known from the IR studies that recovery of the precursor is a minor process upon annealing, and thus, chlorine consumption can be almost entirely be attributed to formation of H−Xe−Cl. After few laser pulses, the H−Xe−Cl absorption is almost completely bleached, and simultaneously, the hydrogen atom absorption regains about 20% of its initial intensity. Similar estimates can be made for the other H−Xe−Y species as well. The corresponding percentages of formation with respect to the initial concentration of Y are: 20% (Y = CN), 28% (Y = Cl), and 24% (Y = Br). The situation is not clear for the Y=I case because the amount of atomic hydrogen was very small, and consequently, only very small amount of iodine was consumed during annealing. The low production yield of atomic hydrogen in this case may be a consequence of the high guest-to-host ratio in this matrix. High precursor concentration favors the formation of protons via ionic channels,[4] and increase the probability for bimolecular formation of molecular hydrogen. The loss mechanisms involved in the photogeneration of hydrogen atoms from HY precursors were recently explored by combining Electron Paramagnetic Resonance (EPR) and luminescence measurements.[32] In light of the present study, the very weak EPR signals of hydrogen observed in Xe matrix may be ascribed to spectral broadening due to highly anisotropic environment.

The formation yields obtained in the present study are systematically somewhat smaller than those given by Pettersson et al.[33] The source for this discrepancy is quite likely related to the matrix preparation conditions, the sample irradiation history, or the excess energy available for the hydrogen in the initial photolysis of the precursor. This excess energy at 6.4 eV excitation is 2.0, 2.6, and 3.3 eV for HCl, HBr, and HI, respectively.[34] A qualitative observation is, indeed, that the obtained yields for formation of H−Xe−Y decrease as a function of the excess energy. At higher excess energies the mean distance between H and Y created by the pholysis is longer, which would in turn yield global mobility and, consequently, more efficient formation of H−Xe−H during annealing. As discussed in ref 33, the H−Xe−Y molecules may also act as intermediates during the photolysis and provide an efficient mechanism for photon induced mobility of hydrogen atoms.

The MRCI caculations for the ground and the first excited states show fairly good agreement with the experimental data. The excitation energies for different halogens are predicted very well. For H−Xe−I, the deviation is somewhat larger than for the others but the direction of the absorption shift is predicted correctly. It is to be noted that the electronic transitions are from a bound ground state to a purely repulsive excited state, which implies that the calculated transition energies are particularly prone to the ground state geometry. The calculated transition moments are exceptionally high, which is fully consistent with the expectations outlined in the previous section. For H−Xe−Cl, the transition can be viewed as a relatively pure intermolecular charge transfer from Cl to H, whereas for Br and I containing molecules, the charge transfer character of the transition gets weaker. The bond lengths for the ground state molecules behave very predictably as a function of electron affinity of the halogen (see Table 1). Finally, on the basis of the present computational data and comparison with results reported by Johansson et al.,[11] we have all reasons to assign the strong UV absorptions to H−Xe−Cl, H−Xe−Br, H−Xe−I, and H−Xe−CN.

Acknowledgment. This study was funded by the Academy of Finland.

References and Notes

(1) Bartlett, N. *Proc. Chem. Soc.* **1962**, 218.
(2) Pauling, L. *J. Am. Chem. Soc.* **1933**, *55*, 1895.
(3) Peterson, K. A.; Petrmichl, R. H.; McClain, R. L.; Woods, R. C. *J. Chem. Phys.* **1991,** *95*, 2352.
(4) Kunttu, H.; Seetula, J. *Chem. Phys.* **1994,** *189*, 273**.**
(5) Beyer, M.; M.; Lammers, A.; A.; Savchenko, E.; E.; Niedner-Schatteburg, G.; G.; Bondybey, V. E. *Phys. Chem. Chem. Phys.* **1999,** *1*, 2213.
(6) Apkarian, V. A.; Schwentner, N. *Chem. Rev.* **1999,** *99*, 481.
(7) Bondybey, V. E.; Räsänen, M.; Lammers, A. *Annu. Rep. Chem. Sect. C*, **1999,** *95*, 331.
(8) For a review, see Pettersson, M.; Lundell, J.; Räsänen, M. *Eur. J. Inorg. Chem.* **1999**, *729.*
(9) Pettersson, M.; Khriachtchev, L.; Lundell, J.; Räsänen, M. *J. Am. Chem. Soc.* **1999**, *121*, 11 904.
(10) Pettersson, M.; Khriachtchev, L.; Lundell, J.; Räsänen, M. *Nature* **2000**, *406*, 874.
(11) Johansson, M.; Hotokka, M.; Pettersson, M.; Räsänen, M. *Chem. Phys.* **1999**, *244*, 25.
(12) Creuzburg, M.; Koch, F.; Wittl, F. *Chem. Phys. Lett.* **1989,** *156*, 387.
(13) Partington, J. R. *General and Inorganic Chemistry*; Macmillan: London, 1946.
(14) (a)Pople, J. A.; Seeger, R.; Krishnan, R. *Int. J. Quantum Chem. Symp.* **1977**, *11*, 149. (b) Krishnan, R.; Schlegel, H. B.; Pople, J. A. *J. Chem. Phys.* **1980**, *72*, 4654. (c) Raghavachari, K.; Pople, J. A. *Int. J. Quantum Chem.* **1981**, *20*, 167.
(15) (a) Knowles, P. J.; Werner, H.-J. *Chem. Phys. Lett.* **1985**, *115*, 259. (b) Werner, H.-J.; Knowles, P. J. *J. Chem. Phys*. **1985**, *82*, 5053.
(16) (a) Werner, H.-J.; Knowles, P. J. *J. Chem. Phys.* **1988**, *89*, 5803. (b) Knowles, P. J.; Werner, H.-J. *Chem. Phys. Lett.* **1988**, *145*, 514. (c) Knowles, P. J.; Werner, H.-J. *Theor. Chim. Acta*, **1992**, *84*, 95.
(17) (a) Blomberg, M. R. A.; Siegbahn, P. E. M. *J. Chem. Phys.* **1983**, *78*, 5682. (b) Langhoff, S. R.; Davidson, E. R. *Int. J. Quantum Chem*. **1974**, *8*, 61.
(18) McWeeny, R. *Methods of Molecular Quantum Mechanics*, 2nd ed; Academic Press: New York, 1992.
(19) Dunning, T. H. Jr. *J. Chem. Phys.* **1989**, *90*, 1007.
(20) (a) Igel-mann, G.; Stoll, H.; Preuss, H. *Mol. Phys.* **1988**, *65*, 1321. (b) Bergner, A.; Dolg, A.; Kuchle, W.; Stoll, H.; Preuss, H. *Mol. Phys.* **1993**, *80*, 1431. (c) Nicklass, A.; Dolg, M.; Stoll, H.; Preuss, H. *J. Chem. Phys.* **1995**, *102*, 8942.
(21) Frisch, M. J.; Trucks, G. W.; Schlegel, H. B.; Scuseria, G. E.; Robb, M. A.; Cheeseman, J. R.; Zakrzewski, V. G.; Montgomery, J. A. Jr.; Stratmann, R. E.; Burant, J. C.; Dapprich, S.; Millam, J. M.; Daniels, A. D.; Kudin, K. N.; Strain, M. C.; Farkas, O.; Tomasi, J.; Barone, V.; Cossi, M.; Cammi, R.; Mennucci, B.; Pomelli, C.; Adamo, C.; Clifford, S.; Ochterski, J.; Petersson, G. A.; Ayala, P. Y.; Cui, Q.; Morokuma, K.; Malick, D. K.; Rabuck, A. D.; Raghavachari, K.; Foresman, J. B.; Cioslowski, J.; Ortiz, J. V.; Stefanov, B. B.; Liu, G.; Liashenko, A.; Piskorz, P.; Komaromi, I.; Gomperts, R.; Martin, R. L.; Fox, D. J.; Keith, T.; Al-Laham, M. A.; Peng, C. Y.; Nanayakkara, A.; Challacombe, M.; Gill, P. M. W.; Johnson, B.; Chen, W.; Wong, M. W.; Andres, J. L.; Gonzalez, C.; Head-Gordon, M.; Replogle, E. S.; Pople, J. A. *GAUSSIAN 98 (Revision A.3)*; Gaussian, Inc.: Pittsburgh, PA, 1998.
(22) Werner, H.-J.; H.-J.; Knowles, P. J.; Amos, R. D.; Bernhardsson, A.; Bering, A.; Celani, P.; Cooper, D. L.; Deegan, M. J. O.; Dobbyn, A. J.; Eckert, F.; Hampel, C.; Hetzer, G.; Korona, T.; Lindh, R.; Lloyd, A. W.; McNicholas, S. J.; Manby, F. R.; Meyer, W.; Mura, M. E.; Nicklass, A.; Palmieri, P.; Pitzer, R.; Rauhut, G.; Schütz, M.; Stoll, H.; Stone, A. J.; Tarroni, R.; Thorsteinsson, T. *MOLPRO package of ab initio programs*, 2000.
(23) Pettersson, M.; Lundell, J.; Räsänen, M. *J. Chem. Phys.* **1995**, *102*, 6423.
(24) Abbate, A. D.; Moore, C. B. *J. Chem. Phys.* **1985**, *82*, 1255.
(25) Lorenz, M.; Kraus, D.; Räsänen, M.; Bondybey, V. E. *J. Chem. Phys.* **2000**, *112*, 3803.
(26) Pettersson, M.; Lundell, J.; Khriachtchev, L.; Räsänen, M. *J. Chem. Phys.* **1998**, *109*, 618.
(27) (a) Fajardo, M. E.; Apkarian, V. A. *J. Chem. Phys.* **1988**, *89*, 4102. (b) Fajardo, M. E. *Thesis*, University of California: Irvine, 1988.
(28) Ault, B. S.; Andrews, L. *J. Chem. Phys.* **1976**, *65*, 4192.
(29) Schallmoser, A. T.; Smith, A. M.; Wurfel, B. E.; Bondybey, V. E.; *J. Chem. Phys.* **1994**, *100*, 5387.

(30) Dunning, T. H.; Hay, P. J. *J. Chem. Phys.* **1978**, *69*, 134.
(31) Eloranta, J.; Kunttu, H. *J. Chem. Phys.* **2000**, in press.
(32) Eloranta, J.; Vaskonen, K.; Kunttu, H.*J. Chem. Phys.* **1999**, *110*, 7917.
(33) Pettersson, M.; Khriachtchev, L.; Roozeman, R.-J.; Räsänen, M. *Chem. Phys. Lett.* **2000**, in press.
(34) Nordling, C.; Österman, J. *Physics Handbook for Science and Engineering*; Studentlitteratur: Lund, 1996.